TECHNICAL REPORTS

nature medicine

Protein microarrays for multiplex analysis of signal transduction pathways

Steven M Chan, Joerg Ermann, Leon Su, C Garrison Fathman & Paul J Utz

We have developed a multiplexed reverse phase protein (RPP) microarray platform for simultaneous monitoring of site-specific phosphorylation of numerous signaling proteins using nanogram amounts of lysates derived from stimulated living cells. We first show the application of RPP microarrays to the study of signaling kinetics and pathway delineation in Jurkat T lymphocytes. RPP microarrays were used to profile the phosphorylation state of 62 signaling components in Jurkat T cells stimulated through their membrane CD3 and CD28 receptors, identifying a previously unrecognized link between CD3 crosslinking and dephosphorylation of Raf-1 at Ser259. Finally, the potential of this technology to analyze rare primary cell populations is shown in a study of differential STAT protein phosphorylation in interleukin (IL)-2-stimulated $CD4^+CD25^+$ regulatory T cells. RPP microarrays, prepared using simple procedures and standard microarray equipment, represent a powerful new tool for the study of signal transduction in both health and disease.

Reversible phosphorylation of proteins by kinases and phosphatases represents a common molecular mechanism by which intracellular signals are transmitted. With over 2,000 human genes predicted to code for kinases[1] and the potential for each kinase to act on multiple targets, signaling networks are immensely complex. An important step toward unraveling this complexity is the development of new proteomics technologies that can quantitatively monitor the phosphorylation states of signaling proteins in a multiplex fashion. Such technologies would enable the detailed, global analysis of signaling pathways, and the rapid identification of previously unrecognized signaling events. In this report, we describe the development of a flexible protein microarray platform for monitoring protein phosphorylation and its application in the study of T-cell signaling.

Microarrays offer a convenient platform for multiplex protein analysis as shown by our recent success in using autoantigen microarrays for profiling serum autoantibodies[2,3]. Approaches that rely on immobilized antibodies to capture their analytes from solution (forward phase approach) are constrained by the lack of antibodies that function in this format[4–6]. Furthermore, the detection of bound proteins can be problematic as protein labeling with fluorescent dyes has the potential to mask critical binding epitopes[6]. A need for relatively large amounts of starting material also makes this strategy impractical for studying rare cell populations. We therefore explored the utility of RPP microarrays, initially described by Paweletz *et al.* to study frozen tissue samples[7]. RPP microarrays are fabricated by depositing small volumes of cell lysates onto a high protein-binding substratum using a robotic microarrayer. Each cell lysate microspot contains the full complement of intracellular proteins and phosphorylated analytes from that sample. Arrays are probed with signal-generating detection antibodies, which can either be phosphorylation state–dependent or independent. The signal intensity of each microspot correlates with the abundance or level of phosphorylation of the analyte[8,9]. Because thousands of samples can be spotted in high density onto a single slide, a large number of samples can be monitored simultaneously, thereby increasing throughput and simplifying crosscomparisons between samples.

The development and application of RPP microarrays for large-scale analysis of signal transduction in stimulated living cells have not yet been described. The use of living cells is clearly required for mapping the normal signaling pathways downstream of an environmental stimulus. Moreover, abnormal cells may require environmental stimulation to reveal cryptic signaling signatures that would otherwise be overlooked in an unstimulated state[10]. Here we present generally applicable methods for the study of signal transduction in living cells using RPP microarrays.

RESULTS

Design and fabrication of RPP microarrays

To fabricate RPP microarrays, we used a contact-printing robotic microarrayer fitted with solid pins to deliver nanoliter volumes of whole cell lysates onto nitrocellulose-coated slides. The resulting features measured approximately 400 μm in diameter. After blocking, we probed slides with either phospho-specific or pan-specific primary antibodies, which were subsequently detected with a horseradish peroxidase–linked secondary antibody. To amplify the signal, we took advantage of tyramide signal amplification technology in which horseradish peroxidase catalyzes the deposition of a biotinyl-tyramide conjugate onto the slide[11]. Bound biotin was detected with Cy3-labeled streptavidin and fluorescence intensity measured using a microarray scanner. Because variations can occur during spotting and sample preparation, we normalized the signal intensity of each spot to

Division of Immunology and Rheumatology, Department of Medicine, Stanford University School of Medicine, Stanford, California 94305, USA. Correspondence should be addressed to P.J.U. (pjutz@stanford.edu).

Published online 21 November 2004; doi:10.1038/nm1139

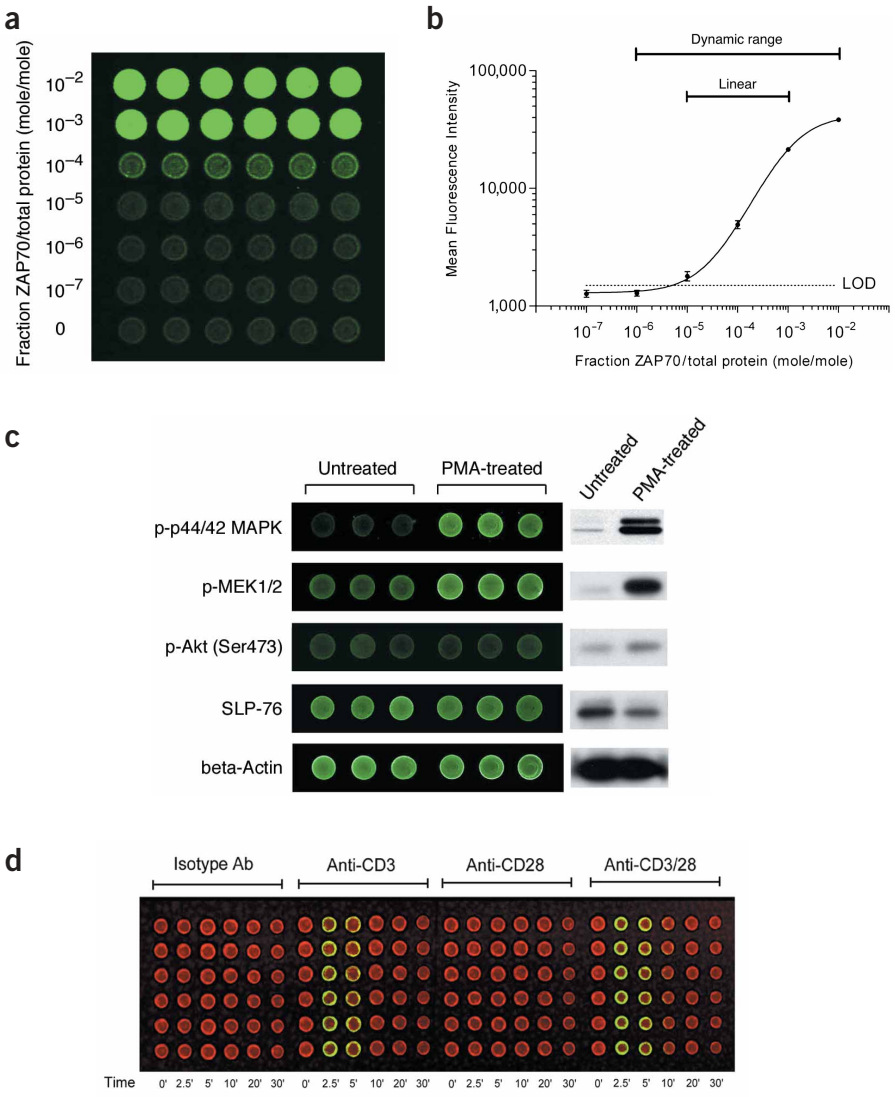

Figure 1 RPP microarray performance characteristics and validation. (**a**) Fluorescent image of an array spotted with A431 lysates spiked with tenfold dilutions of ZAP70 and probed with a ZAP70 specific antibody. Six replicates were spotted across each row. Green signal (Cy3) corresponds to the level of ZAP70. (**b**) Quantitative analysis of the above array. LOD denotes limit of detection. Mean ± s.d. values are graphed. (**c**) Detection of epitope-specific phosphorylation in PMA-treated versus untreated serum-starved Jurkat T cells using RPP microarrays. Corresponding immunoblots of the same samples are shown on the right panel. Antibodies specific for p44/42 MAPK, MEK1/2 and Akt are phospho-specific. Antibodies specific for SLP-76 and β-actin are phosphorylation state–independent. (**d**) Detection of p44/42 MAPK phosphorylation in Jurkat T cells stimulated with the indicated crosslinking antibodies. Six replicates of each sample were spotted down each column. Green signal (Cy3) corresponds to p44/42 MAPK phosphorylation. Red signal (Cy5) corresponds to β-actin levels.

the level of β-actin, which serves as an internal marker for total protein deposited. In some experiments, we controlled for changes in analyte abundance by calculating the ratio of normalized signals for phospho-specific and pan-specific antibodies.

Performance characteristics of RPP microarrays

To test the sensitivity, dynamic range and signal reproducibility of the arrays, we generated microarrays spotted with lysates from an epidermoid carcinoma cell line (A431) spiked with a T cell–specific protein, ZAP70, over a range of tenfold dilutions and probed the arrays with a ZAP70 antibody (**Fig. 1a**). Assuming an average molecular weight of 60 kDa for cellular proteins, we determined the limit of detection to be between 1 in 10^5 to 10^6 in mole fraction (ZAP70/total protein) (**Fig. 1b**), permitting the detection of phosphorylated targets that are present at ~1,500 copies per cell (assuming 100 pg of protein per cell). Quantitative analysis showed a dynamic range of about four logs and within this range, a two-log linear response (**Fig. 1b**). The coefficient of variation within the replicated spots was less than 10% for all replicates analyzed. Although each antibody is unique in its binding affinity for its cognate antigen, the performance characteristics observed with this ZAP70 antibody are representative of three other antibody-antigen pairs we similarly tested (data not shown).

Detection of epitope-specific phosphorylation

We generated microarrays composed of lysates from either phorbol 12-myristate 13-acetate (PMA) treated or untreated Jurkat T cells and probed them with a panel of phospho-specific antibodies. PMA is known to directly activate several isoforms of protein kinase C (PKC) leading to the rapid phosphorylation of MEK1/2 and p44/42 MAPK. Phosphorylation of Akt/protein kinase B, which is not directly linked to PKC-dependent pathways, is not affected (**Fig. 1c**). Corresponding immunoblots confirmed the results obtained using RPP microarrays (**Fig. 1c**). Phosphorylation state–independent antibodies against SLP-76 and β-actin showed no changes in the abundance of these two proteins, confirming the specificity of the observed changes in phosphorylation in MEK1/2 and p44/42 MAPK.

To study physiologically relevant phosphorylation events, we activated Jurkat T cells with CD3 and CD28 antibodies, mimicking stimulation through the T-cell receptor (TCR) and costimulation receptor CD28, respectively. Lysates generated from stimulated cells over a 30-min time course were used to fabricate RPP microarrays. A representative image of such an array probed with a phospho-p44/42 MAPK antibody shows an increase in phosphorylation following stimulation with CD3 or CD3 + CD28 (**Fig. 1d**). The intensity of Cy3 (green) fluorescence corresponds to the level of p44/42 MAPK phosphorylation. This intensity is ratiometrically normalized to Cy5 (red) fluorescence, which corresponds to the level of β-actin within the feature.

Analysis of signal transduction kinetics

RPP arrays were used to profile the kinetics of phosphorylation of phospholipase C (PLC) γ1 on Tyr783 in Jurkat cells activated through

CD3 and CD28 receptors. Phosphorylation by Syk at Tyr783 activates the enzymatic activity of PLCγ1 and thus serves as a useful indicator of PLCγ1 activity[12]. Lysates from Jurkat T cells stimulated with varying combinations of antibodies to CD3, CD28 and isotype controls were collected over a 30-min period, arrayed and probed with a phospho-PLCγ1 (Y783)-specific antibody (**Fig. 2a**). To obtain ratiometric data normalized to total PLCγ1 level, we probed an identical array with a pan-specific PLCγ1 antibody (**Fig. 2a**) and calculated the ratio of phospho-PLCγ1 to total PLCγ1 (**Fig. 2a**). CD3 crosslinking alone resulted in a rapid increase in the level of PLCγ1 phosphorylation within the first 2.5 min of stimulation. This level of phosphorylation quickly diminished to baseline by 10 min. Stimulation with CD28 alone contributed to a lesser but sustained increase in PLCγ1 phosphorylation lasting at least 30 min. In combination with CD3 crosslinking, costimulation with CD28 prevented the level of phosphorylation from diminishing to baseline and maintained it at a level comparable to that of CD28 stimulation alone. This suggests that stimulation with CD28 + CD3 facilitates optimal T-cell activation by prolonging PLCγ1 activity and enhancing its downstream pathways including NF-AT and PKC activation.

Delineation of downstream signaling pathways

The study of signaling pathways has been greatly aided by cell lines deficient in specific signaling molecules. To show the utility of RPP microarrays in mapping downstream pathways, we stimulated J.gamma1 cells, a mutant line of Jurkat T cells deficient in PLC-γ1, and wild-type Jurkat cells with antibodies to CD3 + CD28 and compared the phosphorylation kinetics of four signaling proteins (**Fig. 2b**). We observed a rapid increase in PLCγ1 phosphorylation within minutes of stimulation followed by a gradual decline in wild-type cells. No change in signal was detected for J.gamma1, confirming its deficiency in the mutant line. The absence of PLCγ1 did not affect the kinetics of Akt phosphorylation at Ser473. In contrast, the rate of dephosphorylation for MEK1/2 and p44/42 MAPK was faster in J.gamma1 cells, although the initial peak in phosphorylation was not appreciably different. These results suggest that PLCγ1 plays a role in sustaining p44/42 MAPK activity during T-cell stimulation, but is dispensable for the initial activation of the ERK kinase pathway. This temporal dependence indicates that at least two distinct mechanisms exist to activate the ERK pathway in T cells.

Multiplex screening of signaling events in T cells

To identify previously unrecognized TCR signaling events, we used RPP microarrays to profile the phosphorylation state of 62 different signaling components in Jurkat T cells stimulated with antibody to CD3 alone or in combination with antibody to CD28. Lysates collected 2.5 min after stimulation with CD3 or CD3 + CD28 were spotted in six replicates onto slides in an 8-plex multi-sector array format and probed with a panel of phospho-specific antibodies (see **Supplementary Fig. 1** online). A database containing all the raw data of two independent screens is located on our lab website.

Stimulation with antibodies to CD3 and CD3 + CD28 resulted in global changes in the phosphorylation state of many signaling proteins (**Fig. 3a**). Phosphorylation events were more common and generally more intense than dephosphorylation events. To identify statistically significant differences, we applied four stringent inclusion criteria to all 62 measurements (see Methods). Of the 62 phosphoproteins probed, 13 experienced a substantial change in phosphorylation with CD3 stimulation alone, and 14 proteins with CD3 and CD28 costimulation (**Fig. 3b**). The two lists overlapped to a large extent, suggesting that the addition of antibody to CD28 does not considerably modify the signaling pathways that become activated shortly after TCR stimulation. We were intrigued by this result because previous studies have shown that phosphorylation of Akt (Ser473), SAPK/JNK and p38 MAPK are enhanced by costimulation in Jurkat cells[13,14]. To test the possibility that CD28 costimulation affects phosphorylation of these signaling proteins at later time points, we performed 30-min kinetic studies examining the phosphorylation of Akt, SAPK/JNK and p38 MAPK (**Supplementary Fig. 2** online). Stimulation with antibodies to CD28 + CD3 enhances phosphorylation of these signaling proteins only after 5–10 min of stimulation. This finding, in combination with our initial observation, suggests

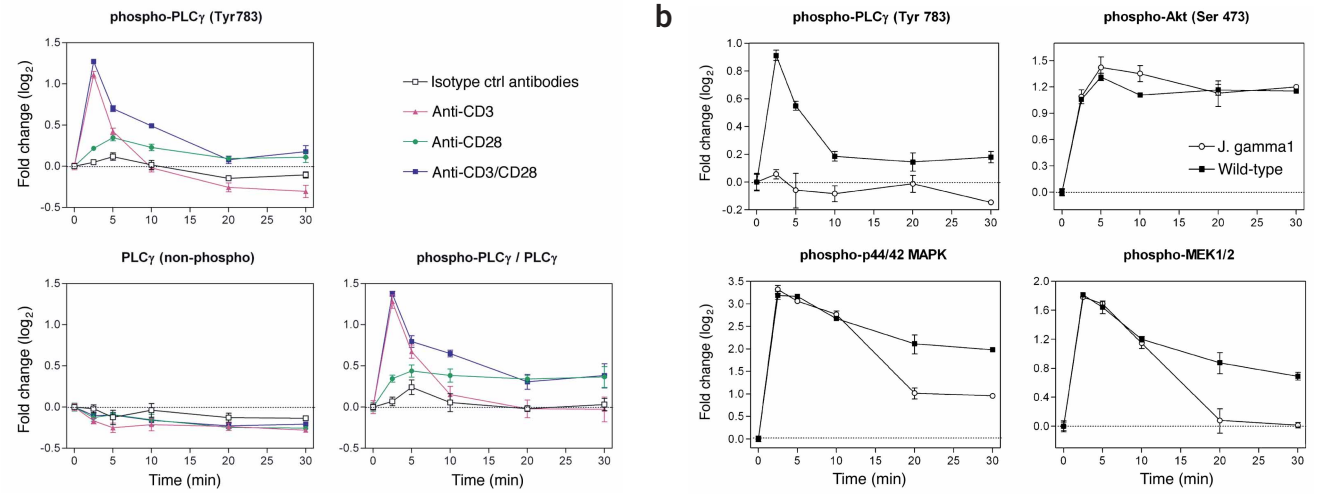

Figure 2 Application of RPP microarrays in the study of signaling kinetics and pathway delineation. (**a**) Kinetics of PLCγ1 (Y783) phosphorylation in Jurkat T cells following stimulation with the indicated antibodies over 30 min. Phosphorylation kinetics unadjusted for total PLCγ1 levels (upper left). Total PLCγ1 levels (lower left). Phosphorylation kinetics adjusted for total PLCγ1 levels (phospho-PLCγ1/total PLCγ1; lower right). (**b**) Phosphorylation kinetics of four signaling proteins (PLCγ1, Akt, MEK1/2 and p44/42 MAPK) in wild-type Jurkat T cells and J.gamma1, a mutant Jurkat line deficient in PLCγ1, stimulated with both antibodies to CD3 and CD28. Both cell lines displayed similar levels of surface CD3 and CD28 as measured by flow cytometry (data not shown). All fold changes are relative to baseline value at time 0. Mean ± s.e.m. values are plotted on all graphs.

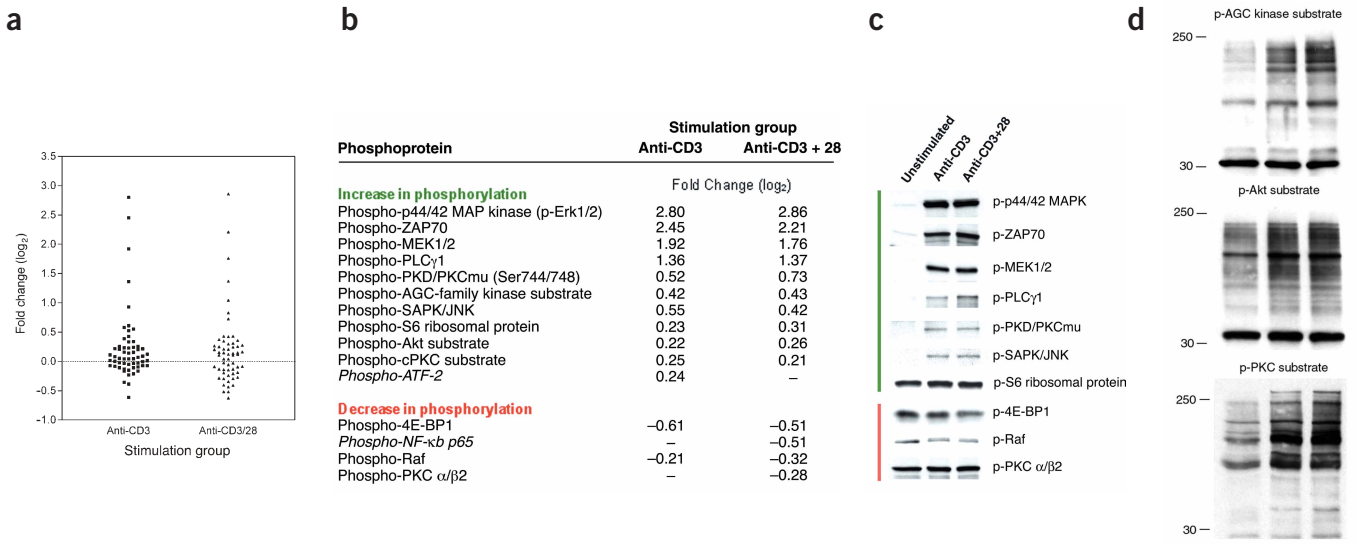

Figure 3 Protein microarray screen with a panel of 62 phospho-specific antibodies. (**a**) Scatter plot of the fold changes associated with stimulation with antibody to CD3 or antibodies to CD3 + CD28 in Jurkat T cells. Each dot represents an individual phosphoprotein measurement. Fold changes are relative to isotype antibody control–treated samples. Only data points with a mean signal-to-noise ratio of greater than 1.3 are plotted. Data points from screen #1 are shown. (**b**) List of phosphoproteins with a substantial change in phosphorylation following stimulation with antibody to CD3 alone or dual stimulation with antibodies to CD3 and CD28. Corresponding immunoblots for phosphoproteins shown in *italics* are absent because bands of the correct molecular weight were not detected for those proteins. '–' denotes that the change in phosphorylation for the phosphoprotein was not found to be significant. Fold changes from screen #1 are listed. (**c**) Corresponding immunoblots for the phosphoproteins on the list. (**d**) For phospho-specific antibodies that recognize phosphorylated substrate motifs, full-length immunoblots are shown. Left to right lane: unstimulated; antibody to CD3; antibodies to CD3 + CD28.

that the effects of CD28 costimulation on TCR signaling are dependent on the duration of receptor stimulation.

To validate the array-determined phosphorylation changes, conventional western immunoblots were performed for individual phosphoproteins (**Fig. 3c,d**). The immunoblot analyses confirmed the phosphorylation changes for all the phosphoproteins except for p-ATF-2 and p-NF-κB p65, which could not be detected by immunoblotting. Many of the phosphoproteins on the list are well known to be involved in TCR signaling, including p44/42 MAPK (Erk1/2), ZAP-70, MEK1/2, PLCγ1 and SAPK/JNK[15], validating the power of this technique. Protein kinase D (PKD/PKC μ) has recently been shown to be activated following TCR stimulation through PKCθ[16,17]. Phosphorylation of S6 ribosomal protein by p70 S6 kinase is correlated with an increase in translational activity, and TCR stimulation activates the enzymatic activity of p70 S6 kinase[18]. Several phospho-specific antibodies recognized phosphorylated substrate motifs of kinases including cPKC, Akt and AGC-family kinases, indicating enhanced activity of these kinases following TCR stimulation. Interestingly, several dephosphorylation events were also detected. An unexpected finding was the dephosphorylation of Raf-1 at Ser259, which has not been previously reported to be associated with TCR stimulation. Phosphorylation at Ser259 negatively regulates Raf-1 activity since mutation of Ser259 to alanine generates a constitutively active kinase[19]. Furthermore, Akt inhibits Raf-1 activity by phosphorylating Ser259 (ref. 20). The precise mechanism by which Ser259 phosphorylation downregulates Raf-1 activity is unclear. Nevertheless, the dephosphorylation of Raf-1 at Ser259 by TCR stimulation is consistent with the fact that the ERK/MAPK pathway, which requires Raf-1 activity for optimal activation, is strongly stimulated upon TCR crosslinking.

Because Raf-1 is the upstream kinase of MEK, we further investigated whether the dephosphorylation of Raf-1 coincided with its abil-

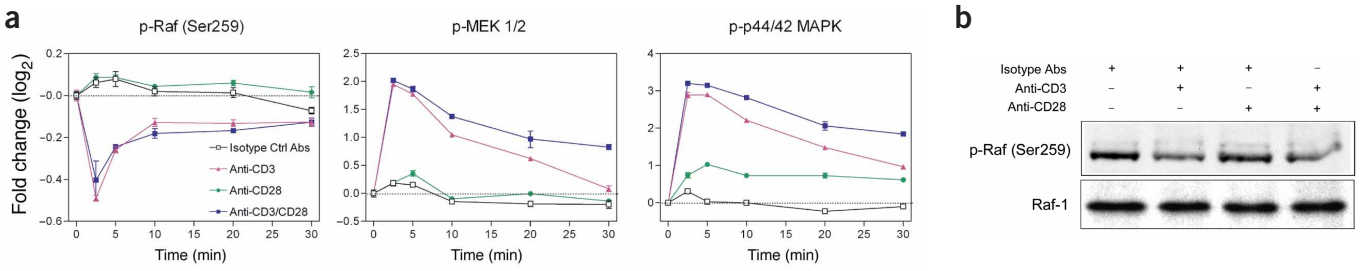

Figure 4 CD3 crosslinking induces Raf-1 Ser259 dephosphorylation in both Jurkat and primary human T cells. (**a**) Kinetics of phosphorylation of Raf-1 Ser259, MEK1/2 and p44/42 MAPK following CD3, CD28, CD3 + CD28 or isotype antibody control stimulation. Raf-1 dephosphorylation coincides with MEK1/2 phosphorylation and activation. All fold changes are relative to baseline value in time 0. Mean ± s.e.m. values are plotted on all graphs. (**b**) Peripheral human T lymphocytes were isolated and stimulated with the indicated antibodies for 20 min. Equal amounts of lysate were loaded in each lane. Immunoblots for phosphorylated Raf-1 (Ser259) and total Raf-1 are shown.

ity to phosphorylate MEK1/2. We used RPP microarrays to profile the phosphorylation kinetics of Raf-1, MEK1/2 and p44/42 MAPK in parallel over a 30-min stimulation period (**Fig. 4a**). We observed that Ser259 dephosphorylation occurred rapidly following stimulation with antibody to CD3 and peaked at 2.5 min. Ser259 was partially dephosphorylated during the next 5–10 min and maintained a sub-baseline level of phosphorylation for the remaining stimulation period. CD28 crosslinking alone had no appreciable effect on Ser259 dephosphorylation. Even in the setting of costimulation, Raf-1 dephosphorylation was insensitive to signals emanating from the CD28 receptor. The kinetics of MEK1/2 and p44/42 MAPK phosphorylation followed closely with that of Raf-1 dephosphorylation, suggesting that Raf-1 activity is regulated through Ser259 phosphorylation. To confirm that this signaling event is a genuine physiological response in normal T cells, we stimulated purified peripheral human T lymphocytes with antibodies to CD3 and CD28 and determined the level of Ser259 phosphorylation through immunoblotting. A similar response was observed in primary T cells when stimulated for 20 min (**Fig. 4b**). Surprisingly, no dephosphorylation was observed with a 5-min stimulation (data not shown), suggesting that the kinetics of dephosphorylation may be faster in transformed leukemic cells. It is unclear how TCR stimulation leads to Raf-1 dephosphorylation, although protein phosphatases 1 and 2A are likely to be involved[21].

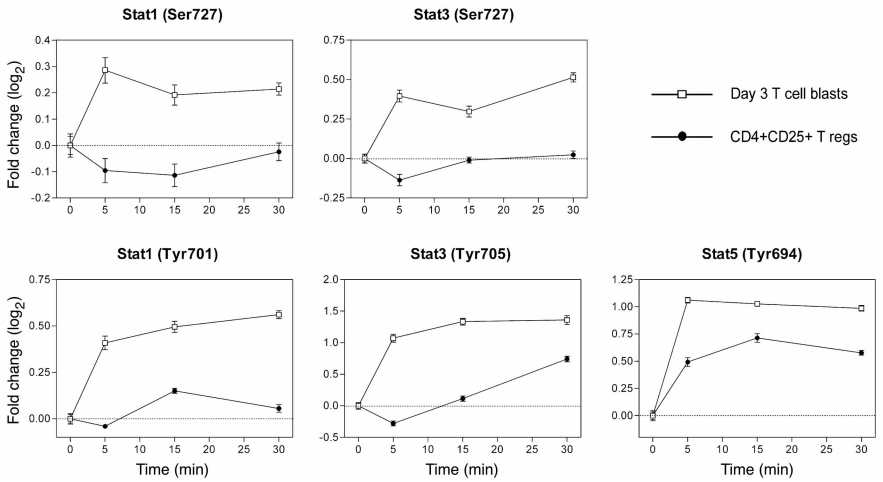

Figure 5 Differential STAT protein phosphorylation in IL-2-stimulated $CD4^+CD25^+$ T_R cells. Kinetics of phosphorylation of STAT1, 3 and 5 over 30 min in response to IL-2 stimulation in T_R cells and day 3 T-cell blasts are shown. All fold changes are relative to baseline value at time 0. Mean ± s.e.m. values are plotted on all graphs.

Differential STAT phosphorylation in regulatory T cells

Since the total amount of protein deposited at each microarray feature is estimated to be equivalent to that of ~20 cells, much less than the amount needed for immunoblot analysis, RPP microarrays are ideally suited to study rare cell populations. We used RPP microarrays to analyze signal transduction in highly purified $CD4^+CD25^+$ regulatory T (T_R) cells. T_R cells, which are involved in the active suppression of autoimmune responses, constitute only 5–10% of $CD4^+$ T cells in peripheral lymphoid tissues[22]. A typical purification yields approximately one million cells from the spleen and lymph nodes of one mouse, sufficient for printing thousands of RPP microarray features.

Previous studies have shown that T_R cell numbers are substantially reduced in the peripheral lymphoid organs of mice that lack IL-2 compared with wild-type animals, suggesting that T_R cells require IL-2 signaling for development and/or survival[23,24]. Signaling pathways downstream of IL-2 stimulation in T_R cells are not well characterized. Furthermore, it is unclear whether IL-2 signaling pathways differ between T_R cells and activated $CD4^+$ T-cell blasts, which also express CD25 (IL-2 α-chain). We used RPP microarrays to profile the phosphorylation state of a panel of STAT proteins in T_R cells stimulated with IL-2 and compared the profile with activated $CD4^+$ T-cell blasts.

Arrays fabricated using lysates from IL-2-stimulated T_R cells and T-cell blasts were probed with five phospho-STAT antibodies. Kinetic analysis showed a rapid phosphorylation of STAT1 (Ser 727, Tyr 701), STAT3 (Ser 727, Tyr 705), and STAT5 (Tyr 694) in T-cell blasts within 5 min in response to IL-2 stimulation (**Fig. 5**). We also observed STAT5 phosphorylation in T_R cells stimulated with IL-2, but it was less prominent than that observed in T-cell blasts. In contrast, STAT1 and STAT3 were not phosphorylated in IL-2-stimulated T_R cells (**Fig. 5**). We confirmed results using conventional immunoblots for phosphorylated tyrosine residues (**Supplementary Fig. 3** online). Although STAT5 activity is thought to be necessary for the maintenance of T_R cells in the periphery[25,26], it is not known whether the lack of STAT1 and/or STAT3 activity is associated with their suppressive phenotype. This notable finding may shed light on the signaling pathways that regulate T_R maintenance and function. A large-scale analysis of T_R cell signaling using RPP microarrays is currently underway.

DISCUSSION

Traditional protein analysis methods have provided invaluable insights into signal transduction pathways; however, new proteomics approaches are necessary to unravel the complexity of the largely unexplored signaling network. RPP microarrays represent an exciting, powerful tool for exploring many facets of the network. This technology may also prove to be useful as a high-throughput platform for drug compound screening as shown in a proof-of-concept experiment using well-characterized kinase inhibitors (**Supplementary Fig. 4** online). In addition to the applications described above, RPP microarrays can be used to: (i) analyze the signal transduction pathways of other rare cell populations such as dendritic cells, stem cells or antigen-specific lymphocytes purified using tetramers (ii) identify cryptic signaling pathways or defects revealed by exposing living tumor cells or other diseased tissues to cytokines, chemokines or other bioactive molecules (iii) monitor other stimulus-induced post-translational modification events such as ubiquitination, farnesylation, acetylation, glycosylation and proteolysis using modification-specific antibodies, and (iv) identify stimulus-specific changes in subcellular localization of biomolecules by spotting fractionated cell lysates. By combining genomic profiling technologies with RPP microarray analysis, it should now be possible to piece together the complex pathways connecting the cell surface, genome and proteome in both normal and diseased states.

METHODS

Antibodies. Monoclonal antibody UCHT1 (mouse IgG1, antibody to human CD3ε) and isotype control monoclonal antibodies were purchased commercially (eBioscience). Monoclonal antibody 9.3 (mouse IgG2a, antibody to human CD28) was a gift from C. H. June (University of Pennsylvania Cancer Center).

A complete list of phospho-specific antibodies used in our experiments (Cell Signaling Technologies) is located in **Supplementary Table 1** online. All phospho-specific antibodies were used at a dilution of 1:1,000. Phosphorylation-independent antibodies were used at their recommended dilutions: rabbit antibody to ZAP70 (Cell Signaling Technologies), mouse antibody to SLP76 (BD Biosciences), mouse antibody to β-actin (Sigma), rabbit antibody to pan PLCγ (Cell Signaling Technologies) and antibody to Raf-1 (Santa Cruz). Refer to **Supplementary Note** online for a discussion of antibody crossreactivity.

Cell culture, stimulation and lysate preparation. We cultured Jurkat T cells (clone E6-1) and J.gamma1 in RPMI-1640 supplemented with 10% fetal bovine serum, 2 mM L-glutamine, 25 mM HEPES, 1 mM sodium pyruvate and antibiotics. Cells in logarithmic growth were serum-starved for 6–7 h, washed and resuspended in serum-free RPMI media at 10^7 cells/ml. We treated cells on ice for 10 min with one of four combinations of antibodies: IgG1/IgG2a, antibody to CD3/IgG2a, antibody to CD28/IgG1 or antibody to CD3 and antibody to CD28. The final concentration of each antibody was 5 μg/ml. Antibodies were crosslinked with a donkey anti-mouse IgG secondary antibody (Jackson ImmunoResearch Laboratories) at 10 μg/ml. We initiated stimulation by transferring the cells to a 37 °C water bath. At indicated time points, we lysed aliquots of the cells in an equal volume of 2× lysis buffer: 100 mM Tris pH 6.8, 4% (w/v) SDS, 10% (v/v) glycerol, 2% (v/v) 2-mercaptoethanol, 100 mM NaF, 5 mM EDTA, 5 mM EGTA, 10 mM β-glycerophosphate, 2% (v/v) phosphatase inhibitor cocktail 2 (Sigma), 1× complete protease inhibitor cocktail (Roche). We immediately snap-froze lysates in a dry-ice and ethanol bath to prevent any further changes in phosphorylation. Upon collection of all the samples, we heated the lysates at 100 °C for 10 min, briefly centrifuged them to collect condensation and froze them at –80 °C.

Preparation and stimulation of $CD25^+$ T cells. Six- to ten-week-old female BALB/c mice were killed, spleen and lymph nodes harvested and single cell suspensions prepared. We enriched the samples for $CD25^+$ cells with antibody to CD25 (PC61) - PE + anti-PE magnetic beads using the autoMACS system (Miltenyi Biotech). To obtain $CD4^+CD25^+$ T_R cells, positively selected cells were stained with antibody to CD4 (RM4-5) and FACS sorted to >97% purity. We prepared $CD4^+CD25^-$ cells from the $CD25^-$ negative fraction using CD4 microbeads and the autoMACS system. Day 3 blasts were prepared from $CD4^+CD25^-$ cells by stimulation with 0.5 μg/ml antibody to CD3 in the presence of a tenfold excess of irradiated CD4-depleted lymph node and spleen cells as antigen-presenting cells. We harvested cells after 60 h, purified them on a Lympholyte M gradient (Cedarlane) and rested them in complete RPMI without IL-2 overnight before stimulation. Freshly isolated $CD4^+CD25^+$ T cells and day 3 blasts were stimulated with recombinant mouse IL-2 (50 U/ml, R&D Systems) for 0, 5, 15, 30 min at 37 °C and lysates collected as described above.

Lysate microarray fabrication and processing. We transferred lysates to wells in 384-well polypropylene plates (6–10 μl/well). We used a contact-printing robotic microarrayer (Bio-Rad) fitted with solid spotting pins to spot lysates onto FAST slides (Schleicher & Schuell BioSciences). Slides coated with a single nitrocellulose pad or 8 sectored pads were used depending on the experimental setup. After printing, we blocked slides in a 3% casein solution and probed them overnight at 4 °C with primary antibodies at the appropriate dilution in PBS supplemented with 10% fetal bovine serum and 0.1% Tween-20 (PBST-fetal bovine serum). Arrays were thoroughly washed with PBST and probed with a horseradish peroxidase–conjugated donkey antibody to rabbit IgG secondary antibody (Jackson ImmunoResearch Laboratories) for 45 min. To amplify the signal, slides were incubated in 1× Bio-Rad Amplification Reagent (BAR solution) supplied in the Amplified Opti-4CN Substrate Kit (Bio-Rad) for 10 min at room temperature. The slides were then extensively washed with PBST supplemented with 20% dimethylsulfoxide followed by PBST alone. To detect the bound biotin and β-actin, slides were probed with a mixed solution of Cy3-Streptavidin (Jackson ImmunoResearch Laboratories) and Cy5-conjugated antibody to β-actin for 1 h at 4 °C. The processed slides were scanned using a GenePix 4000A microarray scanner (Axon Instruments) at 10-micron resolution.

Array analysis. We used GenePix Pro 5.0 software (Axon Instruments) to determine the median pixel intensities for individual features and background pixels in both Cy3 and Cy5 channels. We normalized the background-subtracted Cy3 intensities to the level of β-actin (Cy5) at each feature by taking the ratio of Cy3 to Cy5. The mean value of replicate spots was used for all subsequent analysis. For kinetic studies, we calculated fold change with respect to time zero for each time point and displayed change as log base 2 values on the *y*-axis. Two independent 62-phosphoprotein screens were performed. Comparisons were made using the median normalized intensity value of the six replicate features. We considered a change in phosphorylation between the antibody to CD3 or antibody to CD3 + CD28–treated sample and isotype control antibody–treated sample significant if it fulfilled four criteria: (i) mean signal-to-noise ratio for the six replicate features must be greater than 2 (screen #1) or 1.6 (screen #2) (ii) fold change must be greater than 1.15 (iii) statistical significance of the change as calculated using Student's *t*-test must have a $P < 0.05$, and (iv) the observed change must fulfill the above three criteria in both screens.

URL. Utz Laboratory Website: http://www.stanford.edu/group/utzlab

ACKNOWLEDGMENTS

We thank W.H. Robinson and M. Kattah for insightful discussions; and A. Zhang for technical assistance. S.M.C. is supported by the Stanford Medical Scientist Training Program. P.J.U. is supported by grants from the Dana Foundation, Northern California Chapter of the Arthritis Foundation, the Stanford Program in Molecular and Genetic Medicine (PMGM), NIH Grants DK61934, AI50854, AI50865, and AR49328, and NHLBI Proteomics Contract N01-HV-28183.

COMPETING INTERESTS STATEMENT

The authors declare that they have no competing financial interests.

Received 21 April; accepted 29 July 2004
Published online at http://www.nature.com/naturemedicine/

1. Ficarro, S.B. *et al.* Phosphoproteome analysis by mass spectrometry and its application to *Saccharomyces cerevisiae*. *Nat. Biotechnol.* **20**, 301–305 (2002).
2. Robinson, W.H. *et al.* Autoantigen microarrays for multiplex characterization of autoantibody responses. *Nat. Med.* **8**, 295–301 (2002).
3. Robinson, W.H. *et al.* Protein microarrays guide tolerizing DNA vaccine treatment of autoimmune encephalomyelitis. *Nat. Biotechnol.* **21**, 1033–1039 (2003).
4. Nielsen, U.B., Cardone, M.H., Sinskey, A.J., MacBeath, G. & Sorger, P.K. Profiling receptor tyrosine kinase activation by using Ab microarrays. *Proc. Natl. Acad. Sci. USA* **100**, 9330–9335 (2003).
5. Haab, B.B., Dunham, M.J. & Brown, P.O. Protein microarrays for highly parallel detection and quantitation of specific proteins and antibodies in complex solutions. *Genome Biol.* **2**, RESEARCH0004 (2001).
6. MacBeath, G. Protein microarrays and proteomics. *Nat. Genet.* **32** Suppl., 526–532 (2002).
7. Paweletz, C.P. *et al.* Reverse phase protein microarrays which capture disease progression show activation of pro-survival pathways at the cancer invasion front. *Oncogene* **20**, 1981–1989 (2001).
8. Espina, V. *et al.* Protein microarrays: molecular profiling technologies for clinical specimens. *Proteomics* **3**, 2091–2100 (2003).
9. Liotta, L.A. *et al.* Protein microarrays: meeting analytical challenges for clinical applications. *Cancer Cell* **3**, 317–325 (2003).
10. Irish, J.M. *et al.* Single cell profiling of potentiated phospho-protein networks in cancer cells. *Cell* **118**, 217–228 (2004).
11. Bobrow, M.N., Litt, G.J., Shaughnessy, K.J., Mayer, P.C. & Conlon, J. The use of catalyzed reporter deposition as a means of signal amplification in a variety of formats. *J. Immunol. Methods* **150**, 145–149 (1992).
12. Wang, Z., Gluck, S., Zhang, L. & Moran, M.F. Requirement for phospholipase C-gamma1 enzymatic activity in growth factor-induced mitogenesis. *Mol. Cell. Biol.* **18**, 590–597 (1998).
13. Kane, L.P., Andres, P.G., Howland, K.C., Abbas, A.K. & Weiss, A. Akt provides the CD28 costimulatory signal for up-regulation of IL-2 and IFN-gamma but not T_H2 cytokines. *Nat. Immunol.* **2**, 37–44 (2001).
14. Zhang, J. *et al.* p38 mitogen-activated protein kinase mediates signal integration of TCR/CD28 costimulation in primary murine T cells. *J. Immunol.* **162**, 3819–3829 (1999).
15. Cantrell, D. T cell antigen receptor signal transduction pathways. *Annu. Rev. Immunol.* **14**, 259–274 (1996).
16. Matthews, S.A., Rozengurt, E. & Cantrell, D. Protein kinase D. A selective target for antigen receptors and a downstream target for protein kinase C in lymphocytes. *J. Exp. Med.* **191**, 2075–2082 (2000).
17. Yuan, J., Bae, D., Cantrell, D., Nel, A.E. & Rozengurt, E. Protein kinase D is a downstream target of protein kinase C theta. *Biochem. Biophys. Res. Commun.* **291**, 444–452 (2002).

18. Kleijn, M. & Proud, C.G. The regulation of protein synthesis and translation factors by CD3 and CD28 in human primary T lymphocytes. *BMC Biochem.* **3**, 11 (2002).
19. Michaud, N.R., Fabian, J.R., Mathes, K.D. & Morrison, D.K. 14–3-3 is not essential for Raf-1 function: identification of Raf-1 proteins that are biologically activated in a 14–3-3- and Ras-independent manner. *Mol. Cell. Biol.* **15**, 3390–3397 (1995).
20. Zimmermann, S. & Moelling, K. Phosphorylation and regulation of Raf by Akt (protein kinase B). *Science* **286**, 1741–1744 (1999).
21. Jaumot, M. & Hancock, J.F. Protein phosphatases 1 and 2A promote Raf-1 activation by regulating 14–3-3 interactions. *Oncogene* **20**, 3949–3958 (2001).
22. Sakaguchi, S. Naturally arising $CD4^+$ regulatory T cells for immunologic self-tolerance and negative control of immune responses. *Annu. Rev. Immunol.* **22**, 531–562 (2004).
23. Almeida, A.R., Legrand, N., Papiernik, M. & Freitas, A.A. Homeostasis of peripheral $CD4^+$ T cells: IL-2R alpha and IL-2 shape a population of regulatory cells that controls $CD4^+$ T cell numbers. *J. Immunol.* **169**, 4850–4860 (2002).
24. Furtado, G.C., Curotto de Lafaille, M.A., Kutchukhidze, N. & Lafaille, J.J. Interleukin 2 signaling is required for $CD4^+$ regulatory T cell function. *J. Exp. Med.* **196**, 851–857 (2002).
25. Antov, A., Yang, L., Vig, M., Baltimore, D. & Van Parijs, L. Essential role for STAT5 signaling in $CD25^+CD4^+$ regulatory T cell homeostasis and the maintenance of self-tolerance. *J. Immunol.* **171**, 3435–3441 (2003).
26. Snow, J.W. *et al.* Loss of tolerance and autoimmunity affecting multiple organs in STAT5A/5B-deficient mice. *J. Immunol.* **171**, 5042–5050 (2003).